Biology and Medicine

Kamshilin et al., Biol Med (Aligarh) 2016, 8:7
DOI: 10.4172/0974-8369.1000361

Research Article Open Access

Local Thermal Impact on Microcirculation Assessed by Imaging Photoplethysmography

Alexei A Kamshilin[1*], Angelica V Belaventseva[2], Roman V Romashko[2,3], Yuri N Kulchin[2,3] and Oleg V Mamontov[1,4]

[1]*Department of Computer Photonics and Videomatics, ITMO University, Kronverksky Pr, St. Petersburg, Russia*

[2]*Institute for Automation and Control Processes of FEB RAS, Radio St., Vladivostok, Russia*

[3]*Far Eastern Federal University, Sukhanova St., Vladivostok, Russia*

[4]*Almazov Federal Heart, Blood and Endocrinology Center, Akkuratova St., St. Petersburg, Russia*

[*]**Corresponding author:** Dr. Alexei A Kamshilin, Department of Computer Photonics and Videomatics, ITMO University, 49 Kronverksky Pr., St. Petersburg 197101, Russia, Tel: +7 952 261 3784; E-mail: alexei.kamshilin@yandex.ru

Received date: October 18, 2016; **Accepted date:** November 17, 2016; **Published date:** November 24, 2016

Abstract

Laser Doppler Flowmetry and Laser Speckle Contrast Imaging are applied usually for assessment of parameters of the cutaneous blood flow during thermoregulation. Alternatively, this work explores the feasibility of blood pulsation imaging under incoherent green illumination for measuring the response of human body on local thermal impact. The proposed technique allows assessment of the cutaneous blood flow changes during thermoregulation simultaneously in different areas of the body. The preliminary experiments show that the blood pulsation amplitude (BPA) is sufficiently reliable index, which could characterize the relative change of the cutaneous blood flow similarly to the parameter measured with the Laser Doppler Flowmetry technique. It is shown that BPA grows up proportionally to the skin temperature increase in the preliminary cooled finger, whilst it is in the steady state in another finger having the constant temperature. The rate of BPA increase is individual characteristic of a subject, which could serve as a parameter of the subject's vasomotor reactivity on the temperature changes. High quality of visualized distribution of blood pulsations, good repeatability of the BPA, and revealed dependencies of its response on the skin-temperature change offer the prospect for development new system of studying microcirculation.

Keywords: Microcirculation; Thermoregulation; Photoplethysmography; Blood pulsation; Blood perfusion

Introduction

Reaction of blood microcirculation on an external impact is an indicator of injury nervous system [1,2] and vascular disease [3]. Optics has significant potential to provide non-invasive measurement of cutaneous microcirculation. Various optical methods were proposed to assess blood flow: laser doppler flowmetry (LDF), laser speckle contrast imaging (LSCI), optical tomography, polarization spectroscopy, photoplethysmography (PPG), and others [4]. Among these methods, LDF is the most widespread technique for assessment of tissue perfusion. It provides quantitative estimations of relative changes in blood perfusion in response of various external impacts [5-7]. However, LDF probes operate in a single-point, which lead to spatial variability and poor reproducibility of results [8]. These problems were overcame in recently developed systems of laser doppler imaging (LDI), which provide two-dimensional (2D) mapping of cutaneous microcirculation [9,10]. However, LDI systems are either slow [9] when mechanical scanning is used or expensive [10] when scattered light is processed by advanced 2D sensors. Another optical technique widely used for microcirculation visualization is LSCI [11,12]. It is simpler, and it visualizes larger areas of subject's skin than LDI but the perfusion indexes obtained by these two techniques are different [13].

Both LDI and LSCI techniques exploits coherent light source (laser) while there is another optical technology for blood microcirculation assessment, PPG which operates under either incoherent or ambient illumination [14,15]. Since PPG is very simple and cost-efficient technique, it has been widely used in clinical and research settings for continuous and noninvasive monitoring of arterial blood oxygen saturation and heart rate analysis [16]. However, the majority of researchers in the field of photoplethysmography are skeptical in considering the PPG waveform as a reliable indicator of tissue blood perfusion mainly because it is usually spoiled by signal artefacts resulted from motion and low signal-to-noise ratio [17-19]. Exception is the recent work of Abay and Kyriacou in which pulsatile (AC) and slowly varying (DC) components of the PPG waveforms are processed separately to assess blood perfusion via calculation of total hemoglobin [20]. This instrument operates in the reflection mode and provides measurements in a single point (finger) using incoherent illumination at two wavelengths of 660 and 880 nm (red and infrared light) [20]. However, researchers working with imaging photoplethysmography reported that AC-to-DC ratio of the PPG waveform is the highest at green light [21-23] despite of the well-known fact that this light cannot interact with pulsatile arteries because of its small penetration depth [24]. This contradiction was resolved in an alternative model of PPG signal formation recently proposed in our group [25]. It is based on the hypothesis that the light modulation occurs in the capillary bed which is continuously compressed/decompressed by pulsatile arterial pressure [25]. If this hypothesis is true, one can expect that change of cutaneous blood perfusion during thermoregulation could be assessed by measuring parameters of the PPG waveform at green illumination.

In this paper, we present a pilot study reporting on feasibility of measuring the response of human body on local thermal impact by

means of the blood-pulsation-imaging system, which is a particular case of imaging photoplethysmography.

Materials and Methods

Participants and ethics statement

This study was conducted in accordance with the ethical standards laid down in the 1964 Declaration of Helsinki, Guidelines for ethic committees conducting expertise of bio-medical studies of the World Health Organization (WHO) and European Forum for Good Clinical Practice (EF GCP). The study plan was approved on 15.02.2016 by the Bio-Medical Ethics Committee, Far-Eastern Federal University, Vladivostok, Russia. The experiments were conducted at the Institute of Automation and Control Processes FEB RAS, Vladivostok, Russia. Measurements were carried out with 9 healthy subjects (7 males and 2 females) aging 21-29 years (Table 1). Nobody of them had suffered from cardiovascular disease or diabetes mellitus. The content of the research was explained to the subjects prior to the study and their informed consent was obtained in written.

Subject	Body temp, °C	Finger temp, °C	Heart rate, bpm	Height, cm	Weight, kg	Age, years
S1	36.6	33.1 ± 0.5	73	188	74	23
S2	36.6	33.8 ± 0.5	59	183	76	23
S3	36.6	32.2 ± 0.8	68	183	69	24
S4	36.6	32.4 ± 1	62	185	72	27
S5	36.7	33.7 ± 0.2	51	164	58	23
S6	36.7	34 ± 0.4	66	177	80	21
S7	36.6	33 ± 0.8	70	182	103	28
S8	36.6	31.7 ± 0.5	67	172	69	29
S9	36.4	29 ± 1	69	162	67	25

Table 1: Subjects participated in the study.

Blood pulsation imager

Layout of the measurement system, which consists of an illuminator and a digital camera, is shown in Figure 1. Continuous video recording of the subject's palm was carried out in the reflection mode through the glass plate with which the palm was in the physical contact. Contact with the glass plate had a double goal. First, it stabilized the image by diminishing accidental motion artifacts. Second, it significantly increased the PPG amplitude due to a larger modulation amplitude of the capillary density by pulsating arteries [25,26]. Both the illuminator and digital camera were situated under the glass plate. Two identical light-emitting diodes (LED) operating at the wavelength of 525 nm with the spectral width of 40 nm and output power of 5 W were used to provide uniform illumination of the palm. A focused image of the palm was formed in the complementary metal-oxide semiconductor (CMOS) sensor of a black-and-white camera (12-bit model uEye UI-3360CP-NIR-GL of Imaging Development Systems GmbH) by a lens of TECHSPEC®VIS-NIR (C Series, f=35 mm, NA=0.021) after reflection from the tilted mirror as shown in Figure 1. Video frames with pixel resolution of 1024 × 460 were recorded at the frequency of 30 frames per second during 120 seconds. To diminish the influence of light reflections from the glass interfaces and subject's skin, we used the polarization filtration technique [27]. To this end, the light of each LED passed through a thin-film polarizer, whereas one more polarizer was attached to the camera lens. Transmission axes of the camera- and LEDs polarizers were adjusted to be mutually orthogonal. The distance between each LED and the palm was about 21.5 cm whereas the camera was installed at the distance of 72 cm from the palm.

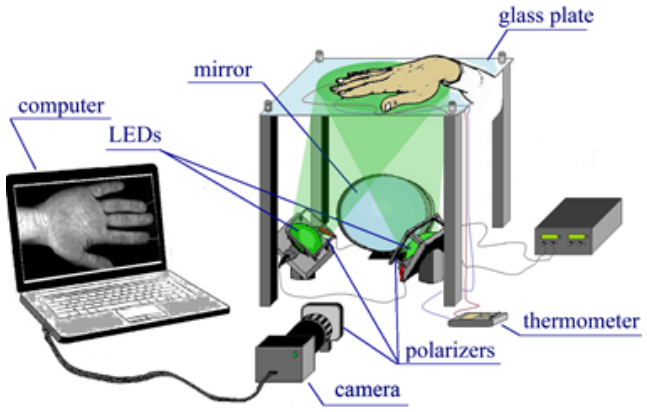

Figure 1: Schematic view of the blood pulsation imaging system. LEDs are light-emitting diodes operating at the wavelength of 525 nm. Thermometer records the skin temperature in the distal phalanx of the index and ring fingers.

Two thermocouples were embedded in the glass plate to measure continuously the skin temperature in the distal phalanx of the index and ring fingers when they contacted the glass. The temperature data were read out at the frequency of 2 Hz. Video and temperature recordings started prior the subject put his palm onto the glass plate. All video frames were saved on a laptop computer in the portable network graphics (PNG) format together with the temperature data for further processing. All measurements were carried out in a laboratory without ambient illumination, maintained at a temperature of about 23°C and relative humidity of 30-50%.

Experimental protocol

At the preparation stage, a distal phalanx of subject's index finger was cooled down by immersing into a mixture of ice and water at the temperature of 5°C for 60 ± 2 seconds. The rest of the palm was not cooled. After the finger cooling, the whole palm was led into the contact with the glass plate having the room temperature of 23°C. During the video recording, a subject was asked to sit comfortably, avoid any movement, keep silence, and breathe evenly. The process of the finger's warming was recorded during 120 seconds. Thereafter, a subject was sat at the relaxed position at least 10 minutes before began the similar procedure of measurements by cooling the same index finger. We carried out 6-8 trials of the finger's cooling/warming for each subject.

Data processing

The recorded video frames were processed offline by using custom software implemented in the MATLAB® platform. At the first step of the algorithm, we calculated the spatial distribution of the blood pulsations amplitude (BPA) by using synchronous amplification of the recorded frames with the heartbeat frequency, which was described in details in our previous papers [21,28]. Briefly, the technique includes the following steps. (A) Finding the beginning and duration of each cardiac cycle from frame-to-frame evolution of the mean pixel value in a region of 11 × 11 pixels (2.5 × 2.5 mm^2) situated in the distal phalanx of the long finger. (B) Using these data for defining the complex reference function of the sinusoidal type for every cardiac cycle, which is required for lock-in amplification [28]. (C) Calculating a correlation matrix between each pixel intensity in the frame and the reference function for each cardiac cycle. The modulus of the correlation matrix represents the spatial distribution of BPA as the AC/DC ratio measured in percent [28]. The set of correlation matrices calculated for each cardiac cycle shows BPA evolution in time and space. Examples of BPA distribution at the beginning and end of the trial are shown in Figures 2a and 2b, respectively. To increase the signal-to-noise ratio, distributions in Figure 2 were averaged over four consecutive cycles.

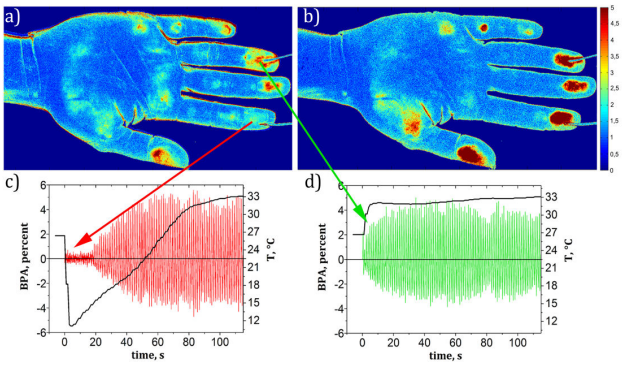

Figure 2: Maps of the blood pulsation amplitude of the subject's palm at the beginning (a) and at the end (b) of the experiment. Evolution of the PPG waveform calculated at the "hot" spots of the preliminary cooled (c) red curve and non-cooled (d) green curve finger accompanied by the respective evolution of the skin temperature shown by the black curve. The color scale on the right of the maps shows BPA as the AC/DC ratio in percent.

At the second stage of the algorithm, two Regions of Interest (ROI, size of 11 × 11 pixels) were chosen nearby the temperature sensors. Frame-to-frame evolution of the mean pixel intensity in the selected ROIs was typical for a PPG signal with pulsatile AC and slowly varying DC components [16,18,21]. By calculating AC/DC ratio, we compensated non-uniformity of the palm illumination. After inverting the sign of the AC/DC ratio, the PPG waveform, which positively correlates with changes of the arterial blood pressure, was calculated. An example of the PPG waveform in the ROI placed in the distal phalanx of the precooled finger is shown in Figure 2c. It was found that the blood pulsations amplitude in this finger grows up with the finger's warming in all studied subjects. However, this growth started always with the delay of 5-25 seconds after the moment of the palm-glass contact. The rate of the BPA growth was estimated as the difference between the PPG-waveform amplitudes in the starting moment of growing and after ten seconds normalized to the skin-temperature difference during the same period.

Results

Dynamics of BPA maps

Spatial distribution of the blood pulsation amplitude for one of the subjects at the beginning of a trial (at the third second after the palm contacted the glass) is shown in Figure 2a, whereas Figure 2b shows the BPA distribution over the same palm after 99th second. As one can see, blood pulsations are unevenly distributed over the palm with clearly seen "hot" spots of the elevated BPA, which are typically visualized in imaging photoplethysmography when the skin is in the physical contact with the glass [26]. Note that the BPA is very small in the distal phalanx of the index finger (blue color) at the beginning of the trial (Figure 2a) but it grows up at the end of the trial (Figure 2b). Continuous evolution of the PPG waveform during the whole trial in the index finger (which was preliminary cooled) and in the ring finger (without cooling) are shown by the red curve in Figure 2c and by the green curve in Figure 2d, respectively. Colored lines in Figure 2 show the PPG waveforms in two ROIs selected nearby the temperature sensors, while solid black lines show evolution of the skin temperature.

It is seen that BPA of the precooled phalanx gradually grows up during 40 seconds following the growth of the skin temperature. In the ring finger, BPA reaches the steady state much faster after 3 seconds (three cardiac cycles) because the skin temperature of this finger was almost constant during the whole trial. Note that BPA measured in the end of the heating process of the precooled finger for a subject during several trials has satisfactory repeatability: the standard deviation did not exceed 26% of the BPA value averaged over the trials of the same subject.

We found for all studied subjects that the growth of the BPA starts not immediately after the precooled finger contacted the glass plate but with a delay. For better view of the moment when BPA starts to grow, we show the PPG waveform evolution of another subject in Figure 3 with zooming the first 15 seconds in Figure 3b. Note that the skin temperature starts to grow immediately after the contact with the glass, whereas the increase of BPA begins only when the skin temperature reaches 16.2°C. In the set of our 68 experiments, the skin temperature at which BPA starts to grow was found to vary between 12.8 and 18.7°C with the average temperature of 15.9 ± 0.4°C. As it was described in the Sect. 2.4, both PPG waveform and BPA were calculated as the AC/DC ratio of the signal, which is commonly accepted in photoplethysmography [16,18,21]. However, we found that the DC component of the mean pixel-intensity evolution is almost constant before the BPA starts to grow but then it gradually decreases as shown in Figure 3c. Diminishing of the DC component means increase of the light absorption in the skin [16,18]. It may affect the evolution of the PPG waveform as the AC/DC ratio. However, estimations show that the DC-diminishing leads to much smaller BPA growth than simultaneous growth of the AC component: during ten seconds the AC component grows up (7.1 ± 2.5)-fold, whereas the DC component drops down only by 17 ± 6 percent. It means that the temperature-induced increase of the BPA is mainly driven by the growth of the AC component of the PPG waveform.

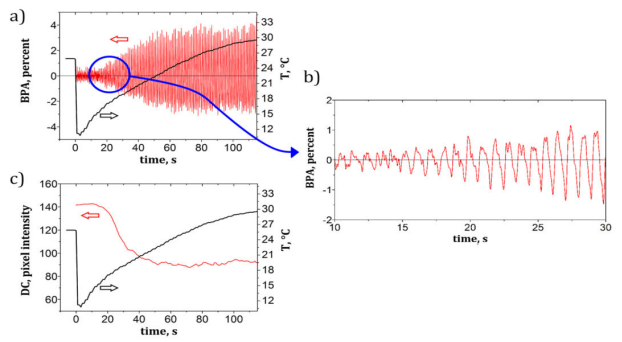

Figure 3: Example of the PPG-waveform evolution and DC-component evolution from the ROI in the precooled finger of the subject S4. (a) The ratio of AC-to-DC components. (b) Zoomed part of the AC/DC evolution from 10 to 30 s. (c) Evolution of the DC-component only. Black lines in parts (a) and (c) show the skin temperature.

Rate of the BPA growth

Linear growth of BPA in the "hot" spot chosen in the precooled finger was observed in all studied subjects. Such a growth always follows the growth of the skin temperature. Therefore, the rate of the BPA growth (in percent per degree) can serve as a parameter of the subject's vasomotor reactivity on the temperature changes. However, we found that this parameter is not exactly the same after its calculation from the different experiments with the same subject. Examples of the rate variations from one experiment to another is shown in Figure 4a for two different subjects. Nevertheless, the mean rate estimated over 6-8 experimental trials for each subject shows that the rate of the individual BPA-growth is different for different subjects as it is shown in Figure 4b.

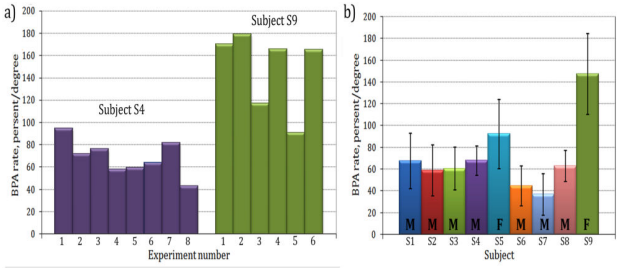

Figure 4: The rate of BPA increase caused by the skin temperature growth for different subjects. (a) Diagram of BPA rate measured in different trials for subjects S4 and S9. (b) Diagram of the BPA rate distribution among the subjects. The bars are the mean values of the BPA rate calculated for the series of different trials whereas the whiskers show the standard deviation from the mean value.

The delay of the BPA growth

It is seen in Figure 3 that the skin temperature starts to grow immediately after the fingers are led to contact with the glass plate. However, blood pulsations become pronounced in the PPG waveform after a certain delay (Figure 3b). Such a delay was observed in all studied subjects. It was varied from 6 to 29 seconds. As seen in Figure 3c, the DC-component does not vary in the same period of the delay, but it drops down simultaneously with the BPA growth. Therefore, the delay of the PPG response can be calculated in two ways: (i) by using change of the AC component, and (ii) by using the DC component. Figure 5 shows distribution of the mean delay time among the all studied subjects estimated from AC and DC components. In all nine subjects, we found significant correlation ($r>0.78$, $p<0.05$) of the time delay calculated by both ways. It is seen in Figure 5 that the time delay is also varied from one subject to another.

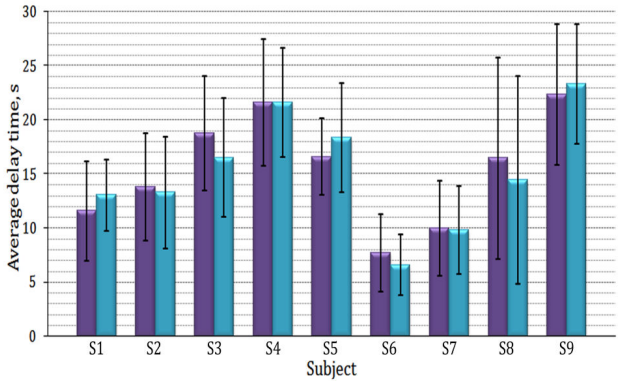

Figure 5: Distribution of the mean delay time between initial moments of the skin-temperature growth and BPA increase among the subjects. Violet bars show the delay measured from the AC-component evolution, whereas blue bars are obtained from the DC-component evolution. Whiskers show the standard deviation from the mean values in series of different trials.

It is worth noting that the rate of the BPA growth (Figure 4b) positively correlates with the delay (Figure 5) of the pulsations appearance in respect with the starting moment of the skin-temperature growth: $r=0.79$, $p=0.01$.

Discussion

Since 1970 up to the present day, the LDF techniques are the most frequently used in the clinical practice for studying the peripheral blood microcirculation [29]. Applications of the LDF and LSCI technologies allows assessment of such important parameters of microcirculation as the velocity of the cutaneous blood flow, the relative laser skin-perfusion units (LSPU), and their variations under different impacts. These parameters are important for estimation of the anatomical and physiological condition, and influence of both local and systemic regulatory mechanisms on the cutaneous blood vessels. It was shown previously that the comparative study using the LDF and LSCI methods reveals correlation of only a part of the parameters of the blood flow relevant to their relative change by an impact. However, the normalization of the obtained parameters to the "biological zero" leads the parameters obtained by two methods to be incomparable [30]. Moreover, the data obtained by using LDF and LSCI methods do not correlate with that obtained by the thermography imaging measurements [31].

The proposed modification of the imaging photoplethysmography technique allows assessment of the cutaneous blood flow changes during thermoregulation simultaneously in different areas of the body. Sufficiently high signal-to-noise ratio (SNR) was achieved in the areas where the subject's skin is contacted with the glass plate. To our mind, the role of the contact is to ensure the conditions for efficient modulation of the capillary bed by arterial pulsations [25,26] and to diminish the motion artefacts influence [27]. The proposed method of the video recording of subject's skin using incoherent green light illumination with appropriate data processing allowed us to visualize areas in which changes of the cutaneous blood flow can be measured with high reliability. The preliminary experiments show that the BPA parameter calculated as the ratio of the AC-to-DC components of the PPG waveform is sufficiently reliable index, which could characterize the relative change of the cutaneous blood flow similarly to the LSPU parameter measured with the coherent laser light. This parameter gives semiquantitative description of the blood flow in the rest but it can be used for studying the body reaction on various stimulus. This statement is supported by the following findings. It was observed that the BPA is kept in the same level in the finger with the stable skin temperature, whereas it increases linearly in the pre-cooled finger (Figure 2). Moreover, BPA changes in the pre-cooled finger correlates with the skin-temperature dynamics. However, this correlation was observed not immediately after the skin temperature starts to grow. In all subjects we observed a delay of the moment at which BPA exceeds the noise level and starts to grow. The delay was found to be an individual characteristic for the subject varying from 6 to 29 s (with the mean value of 15 ± 7 s) both in sequential trials of the same subjects and among different subjects. Surprisingly, the temperature at which BPA starts to grow was almost the same for all subjects (15.9 ± 0.4°C). At the same time, the BPA-growth retardation positively correlates with the BPA-growth rate. Interconnection of these parameters probably shows that both of them depend on the tone of blood vessels.

Therefore, high quality of visualized distribution of blood pulsations, good repeatability of the BPA, and revealed dependencies of its response on the skin-temperature change offer the prospect for development of new system of skin blood flow studying by using blood pulsation imaging approach. The technique is potentially capable to reveal abnormality and/or reactivity of elderly persons and patients with high risk of cardiovascular complication (including metabolic syndrome, diabetes mellitus, rheumatologic and neurologic diseases) on a temperature impact.

One of the limitation of the proposed system is the requirement of the skin-glass contact. At current experiments, the extent of additional pressure applied to the dermis in the place of the contact is not controlled. Such a control would allow improvement of repeatability and fidelity of the measured data. Moreover, further research, which for example may include the study of BPA response on the reactive hyperemia with a local heating after occlusion of the brachial artery [32,33], is needed to determine the range of the BPA dynamics in terms of biological zero and maximal blood flow. Study of the dynamics of the PPG waveform in these conditions is an important step for development of reliable indicators of the cutaneous blood flow and its variability in changeable physiological and pathological conditions.

Acknowledgments

The Russian Science Foundation financially supported the research (Grant 15-15-20012).

Conflicts of Interest

The authors declare no conflict of interest. The founding sponsor has no role in the design of the study; in the collection, analyses, or interpretation of data; in the writing of the manuscript, and in the decision to publish the results.

References

1. Kurvers HAJM, Jacobs MJHM, Beuk RJ, van den Wildenberg FAJM, Kitslaar PJEHM, et al. (1996) The spinal component to skin blood flow abnormalities in reflex sympathetic dystrophy. Arch Neurol 53: 58-65.
2. Yamamoto-Suganuma R, Aso Y (2009) Relationship between post-occlusive forearm skin reactive hyperaemia and vascular disease in patients with Type 2 diabetes--a novel index for detecting micro- and macrovascular dysfunction using laser Doppler flowmetry. Diabet Med 26: 83-88.
3. Ruaro B, Smith V, Sulli A, Decuman S, Pizzorni C, et al. (2015) Methods for the morphological and functional evaluation of microvascular damage in systemic sclerosis. Korean J Intern Med 30: 1-5.
4. Daly SM, Leahy MJ (2013) 'Go with the flow': A review of methods and advancements in blood flow imaging. J Biophotonics 6: 217-255.
5. Maver J, Strucl M (2000) Microvascular reactivity in normotensive subjects with a familial predisposition to hypertension. Microvasc Res 60: 241-248.
6. Tew GA, Klonizakis M, Moss J, Ruddok AD, Saxton JM, et al. (2011) Reproducibility of cutaneous thermal hyperaemia assessed by laser Doppler flowmetry in young and older adults. Microvasc Res 81: 177-182.
7. Bandini A, Orlandi S, Manfredi C, Evangelisti A, Barrella M, et al. (2013) Effect of local blood flow in thermal regulation in diabetic patient. Microvasc Res 88: 42-47.
8. Roustit M, Blaise S, Millet C, Cracowski JL (2010) Reproducibility and methodological issues of skin post-occlusive and thermal hyperemia assessed by single-point laser Doppler flowmetry. Microvasc Res 79: 102-108.
9. Wårdell K, Jakobsson A, Nilsson GE (1993) Laser Doppler perfusion imaging by dynamic light scattering. IEEE Trans Biomed Eng 40: 309-316.
10. Serov A, Steinacher B, Lasser T (2005) Full-field laser Doppler perfusion imaging and monitoring with an intelligent CMOS camera. Opt Express 13: 3681-3689.
11. Forrester KR, Tulip J, Leonard C, Stewart C, Bray RC (2004) A laser speckle imaging technique for measuring tissue perfusion. IEEE Trans Biomed Eng 51: 2074-2084.
12. Draijer M, Hondebrink E, van Leeuwen T, Steenbergen W (2009) Review of laser speckle contrast techniques for visualizing tissue perfusion. Lasers Med Sci 24: 639-651.
13. Binzoni T, Humeau-Heurtier A, Abraham P, Mahe G (2013) Blood perfusion values of laser speckle contrast imaging and laser Doppler flowmetry: is a direct comparison possible? IEEE Trans Biomed Eng 60: 1259-1265.
14. Shelley KH (2007) Photoplethysmography: beyond the calculation of arterial oxygen saturation and heart rate. Anesth Analg 105: S31-S36.
15. Takano C, Ohta Y (2007) Heart rate measurement based on a time-lapse image. Med Eng Phys 29: 853-857.
16. Allen J (2007) Photoplethysmography and its application in clinical physiological measurement. Physiol Meas 28: R1-R39.
17. Sinex JE (1999) Pulse oximetry: principles and limitations. Am J Emerg Med 17: 59-66.

18. Kyriacou PA, Shafqat K, Pal S (2012) Pilot investigation of photoplethysmographic signals and blood oxygen saturation values during blood pressure cuff-induced hypoperfusion. Measurement 42: 1001-1005.
19. Reisner A, Shaltis PA, McCombie D, Asada HH (2008) Utility of the photoplethysmogram in circulatory monitoring. Anesthesiology 108: 950-958.
20. Abay TY, Kyriacou PA (2015) Reflectance photoplethysmography as noninvasive monitoring of tissue blood perfusion. IEEE Trans Biomed Eng 62: 2187-2195.
21. Kamshilin AA, Miridonov SV, Teplov VY, Saarenheimo R, Nippolainen E (2011) Photoplethysmographic imaging of high spatial resolution. Biomed Opt Express 2: 996-1006.
22. Verkruysse W, Svaasand LO, Nelson JS (2008) Remote plethysmographic imaging using ambient light. Opt Express 16: 21434-21445.
23. Sun Y, Papin C, Azorin-Peres V, Kalawsky R, Greenwald SE, et al. (2012) Use of ambient light in remote photoplethysmographic systems: comparison between a high-performance camera and a low-cost webcam. J Biomed Opt 17: 037005.
24. Anderson RR, Parrish JA (1982) Optical properties of human skin. In: Reganand JD, Parrish JA, editors. The Science of Photomedicine. New York: Springer US. pp. 147-194.
25. Kamshilin AA, Nippolainen E, Sidorov IS, Vasilev PV, Erofeev NP, et al. (2015) A new look at the essence of the imaging photoplethysmography. Sci Rep 5: 10494.
26. Kamshilin AA, Mamontov OV, Koval VT, Zayats GA, Romashko RV (2015) Influence of skin status on the light interaction with dermis. Biomed Opt Express 6: 4326-4334.
27. Sidorov IS, Volynsky MA, Kamshilin AA (2016) Influence of polarization filtration on the information readout from pulsating blood vessels. Biomed Opt Express 7: 2469-2474.
28. Teplov V, Nippolainen E, Makarenko AA, Giniatullin R, Kamshilin AA (2014) Ambiguity of mapping the relative phase of blood pulsations. Biomed Opt Express 5: 3123-3139.
29. Stern MD (1975) In vivo evaluation of microcirculation by coherent light scattering. Nature 254: 56-58.
30. Millet C, Roustit M, Blaise S, Cracowski JL (2011) Comparison between laser speckle contrast imaging and laser Doppler imaging to assess skin blood flow in humans. Microvasc Res 82: 147-151.
31. Seifalian AM, Stansby G, Jakson A, Howell K, Hamilton G (1994) Comparison of laser Doppler perfusion imaging, laser Doppler flowmetry, and thermographic imaging for assessment of blood flow in human skin. Eur J Vasc Surg 8: 65-69.
32. Cheng C, Daskalalis C, Falkner B (2013) Non-invasive assessment of microvascular and endothelial function. J Vis Exp 71: e50008.
33. Iredahl F, Lofberg A, Sjoberg F, Farnebo S, Tesselaar E (2015) Non-invasive measurement of skin microvascular response during pharmacological and physiological provocations. PLoS ONE 10: e0133760.